Fusion Alpha Parameters in Tokamaks with High DT Fusion Rates

R.V. Budny[1]

PPPL, Princeton University, P.O. Box 451, Princeton, NJ 08543, USA

(18-Feb-2002)

Abstract Fusion alpha parameters are calculated for Tokamaks with high DT fusion rates using the TRANSP plasma analysis code. Parameters include the fast alpha density, n_α, fast alpha pressure normalized to magnetic field energy, β_α, and its normalized gradient, $-R \times \nabla(\beta_\alpha)$. The plasma conditions are taken from the plasmas in TFTR and JET with the highest DT fusion rates, and from examples proposed for IGNITOR, FIRE, and ITER-FEAT.

1. Introduction

For Tokamaks to become practical sources of energy, large numbers of fusion ions must be confined long enough to heat the plasma. The interactions of fusion alphas on the plasma need to be understood to minimize detrimental effects and exploit beneficial effects. Examples of coupling of fast alphas to the thermal plasma that could be deleterious include stabilization of sawteeth [1,2] and TAE activity [3].

The goal of this paper is to quantify fusion alpha parameters from a selection of proposed "next step" Tokamaks to facilitate assessments of their effects. The first detailed Monte Carlo calculations for IGNITOR, FIRE, and ITER-FEAT are presented. Self-consistent models of the plasmas including their time evolutions are constructed using the TRANSP plasma analysis code [4]. Profiles of alpha parameters, along with the q_{MHD} profiles and MHD equilibria are of use as inputs to codes such as HINST [5] for calculating TAE instability. These results are also of use for codes that calculate the MHD stability and micro-turbulence. Besides the summaries of the alpha parameters given here, electronic files of the MHD equilibria and of the phase space distributions of the fast ions are available.

Another use of these results is in designing experiments to study alpha parameters in burning plasmas. It is likely that auxiliary heating of some form will be used in the next step experiments, but if this generates fast ions (as can ICRH and NBI), these can mask or complicate the measurement of fast alpha effects. One possibility is to abruptly shut off the auxiliary heating in the burning plasma. If the auxiliary ions slow down faster than the alphas, there could be a window of opportunity.

Three proposed Tokamaks are considered, IGNITOR [6], FIRE [7], and ITER-FEAT [8,9]. One plasma from each is chosen for analysis. Ion cyclotron heating is assumed for each, with the ICRH frequency tuned to resonate with the first-harmonic of the He^3 ion-cyclotron frequency and the second-harmonic of T ions near the magnetic axis. In addition, negative-ion NBI is assumed for ITER-FEAT to heat and drive plasma current.

[1]email: budny@princeton.edu

Present-day experiments have produced modest powers from the DT fusion reaction. TFTR achieved 10.3 MW [10] and JET achieved 15.8 MW [11]. The identical analysis techniques are applied to these plasmas for comparing their achieved alpha parameters with those that can be expected from the three next step Tokamaks. One advantage of using the same analysis tools for both present-day experiments and future experiments is that the definitions used for parameters such as triangularity are the same, minimizing the semantic ambiguities in extrapolating from present to future.

2. Analysis Techniques

The TRANSP plasma analysis code [4] is used to analyze the plasmas with the measured or assumed plasma parameters and to calculate the heat deposition profiles. The MHD equilibria are calculated in TRANSP solving the Grad-Shafranov equation. The heat and particle fluxes are calculated from the continuity equations. The fusion ions (and beam ions when NBI is used) are treated using Monte Carlo methods [12] to model their source rates, neoclassical orbits, and slowing-down rates. There are various experimental confirmations of the accuracy of the TRANSP fast alpha calculations [13,14].

The evolution of the q_{MHD} profile is calculated in TRANSP. To model effects of sawteeth, sawteeth crash times are assumed, and the TRANSP sawtooth model is used to helically-mix the plasma current and fast ion profiles. Otherwise, poloidal field diffusion is calculated assuming neo-classical resistivity and driven currents in the case of NBI. All five plasmas studied have conventional, monotonic q_{MHD} profiles, compared in Fig. 1 versus the toroidal flux variable, $x \equiv \sqrt{\text{normalized toroidal flux}}$, which is roughly equal to r/a. Basic plasma conditions of the plasmas are summarized in Table 1.

The ICRH power deposition profiles are computed, using the SPRUCE full wave, reduced-order package [15] in TRANSP. For the next step Tokamaks, a relatively close-fitting antenna is assumed, with a strap separation of 30 cm. The relative phasing of the straps is assumed to be π.

The accumulation of alpha ash in FIRE and ITER-FEAT is simulated by assuming a constant diffusivity and no pinch. The recycling coefficient of the He is assumed to be 20 %. Low (pessimistic) values for the diffusivity are assumed, but accumulation in the plasmas does not reduce the DT fusion yield significantly.

3. Empirical energy confinement scaling laws

The next step plasmas are very different from present day plasmas in many ways, but comparisons of their performance with empirical scaling laws could be useful for assessing the likelihood of being able to produce the plasmas. Several empirical scaling laws for the thermal energy confinement time have given accurate fits to existing data. One is the fit for ELMy H-mode plasmas [16]:

$$\tau_{IPB98y} = 0.144 I_p^{0.93} R^{1.39} a^{0.58} \bar{n}_e^{0.41} B_{Tor}^{0.15} A_h^{0.19} \kappa^{0.78} P_{heat}^{-0.69} \qquad (1)$$

Here I_p is the plasma current [MA], $\bar{n}_e$ is the line-averaged electron density [$10^{20}/m^3$], B_{Tor} is the toroidal magnetic field [T], A_h is the volume-averaged isotopic mass of the hydrogenic species, and P_{heat} is the total heating of the thermal plasma [MW]. Generally

P_{heat} is assumed to be the external heating plus the alpha heating when applicable, but the definition used here is slightly lower for the TFTR and JET plasmas which have non-negligible losses of fast ions (shine-through, orbits intercepting objects, stochastic toroidal field ripple, charge-exchange). Thus the definition of τ_{ITB98y} used here is slightly higher than the usual definition.

This fit is not applicable to TFTR supershots or to the JET Hot-Ion H-mode plasma, but it agrees surprisingly well with the thermal energy confinement time (at the boundary), $\tau_{E,th}(1)$, as seen in Table 1. The fit is more relevant for comparison with the values calculated for the ELMy H-mode plasmas assumed for FIRE and ITER-FEAT plasmas. The estimate of energy confinement time given by the ratio of the total stored energy and the heating power is higher than $\tau_{E,th}(1)$, since all the plasmas contain fast ion contributions to the total energy.

There are other features of ELMy H-mode plasmas that effect their energy confinement. They tend to have higher energy confinement when the triangularity of their boundary, $\delta(1)$, is large, and when their electron density profile is more peaked. They tend to have lower confinement when $\bar{n}_e$ is high (or very low) relative to the Greenwald density defined as $n_{GW} = I_p/(\pi a^2)$ $[MA/m^2]$. An empirical correction factor that accounts for these effects is given in [17]:

$$f = 0.71 + 0.33\delta(1) - 1.58(f_{GW} - 0.63)^2 + 0.58(\bar{n}_e/n_{ped} - 1) \qquad (2)$$

where $f_{GW} = \bar{n}_e/n_{GW}$ and n_{ped} is the electron density at the top of the pedestal. The corrected fit for the confinement time is the product $f\tau_{IPB98y}$.

Another parameter listed in Table 1 is the L-mode [16] fit to τ_E for L-mode plasmas:

$$\tau_L = 0.0578 I_p^{0.96} R^{1.89} a^{-0.06} \bar{n}_e^{0.40} B_{Tor}^{0.15} A_h^{0.20} \kappa^{0.64} P_{heat}^{-0.73} \qquad (3)$$

Table 1 shows that τ_L is about τ_{IPBy} / 2 for the plasmas considered.

4. Plasma and alpha parameters

0.1 TFTR

The TFTR plasma was a supershot [10] achieved with extensive wall conditioning and injection of Li pellets into the Ohmic phase to reduce the influx of hydrogenic and impurity ions. The auxiliary heating consisted of 25.3 MW of T-NBI and 14 MW of D-NBI. The plasma experienced a minor disruption late in the flattop, followed by a carbon bloom, probably caused by a flake or limiter dust entering the plasma. This event caused the total number of electrons in the plasma to increase by a factor of 2.6 in 200 msec, increasing f_{GW} from 0.46 to nearly 1.0, while broadening the density profile considerably. With the decreased slowing down time, the alpha heating power increased about 30 % during the bloom, and $\max\{P_\alpha/P_{heat}\}$ increased by a factor of three. Due to the need for steady state conditions in a reactor, the parameter values are quoted in Table 1 just before the bloom.

Profiles of the plasma parameters in TFTR before the bloom are shown in Fig. 2. The profile for the anomalous heat conduction, $\chi_{\rm eff}$, rises steeply from the core to the edge,

and is near 1.5 [m^2/s] at the mid-radius ($x = 0.5$). Time evolutions of selected plasma parameters are shown in Fig. 3. Table 1 gives a summary of some parameters of use for quantifying effects of alpha particles effects such as the slowing down time (for energy to slow to 1.5 T_i) in the center.

0.2 JET

The JET plasma was a hot-ion H-mode [11] achieved by starting with a relatively low-density Ohmically-heated plasma. The auxiliary heating consisted of 11.9 MW D-NBI, 10.5 MW T-NBI, and 3 MW ICRH tuned to resonate with hydrogen-minority ions near the plasma axis. The plasma energy increased throughout an ELM-free period lasting 0.9 s. Then a series of three giant ELMs occurred. The values of the alpha parameters quoted in Table 1 are at 13.35 s, just before the first giant ELM, and the end of the charge-exchange spectroscopy data. Higher values are recorded [18] 100 msec after the first giant ELM; however the giant ELMs do not appear compatible with practical reactors.

Input parameters and results of the ICRH modeling are summarized in Table 2. Profiles of the plasma parameters just before the first giant ELM are shown in Fig. 4. The profile for $\chi_{\rm eff}$ is relatively flatter than that for the TFTR supershot, and is near 0.4 [m^2/s] at the mid-radius. Time evolutions of some of the plasma parameters are shown in Fig. 5.

0.3 IGNITOR

IGNITOR [6] is designed to have a high toroidal field with normal-conducting magnets, so the plasma durations will be relatively short. It is not designed to have a divertor, so the plasma boundary will be shaped by limiters. High plasma current and high electron density with a peaked profile are assumed. Some of the plasma parameters differ slightly from those given in Ref. 6. Profiles during the flattop are shown in Fig. 6. Since the limiters are designed to be made of graphite, the dominant impurity species is assumed to be carbon with the $Z_{\rm eff}$ profile shown in the Figure.

Although Ohmic ignition is envisioned, the case considered here has 24 MW of He^3-minority ICRH. Two frequencies are assumed, 12 MW at 120 MHz and 12 MW at 140 MHz to resonate near the magnetic axis both during the ramp up of the toroidal field, and the flattop. A contour plot of the power deposition is shown in Fig. 7. The value computed for $\tau_{E,th}(1)$ is larger than the L-mode fit, τ_L, but below the ELMy H-mode fit τ_{IPB98y}. Thus the assumed profiles and heating do not reflect the possibility of a dramatic enhancement of confinement that could result from extremely high $n_e(0)$ and peakedness.

The assumed time evolutions for the plasma parameters are shown in Fig. 8. The computed value for $\chi_{\rm eff}$ is near 6 [m^2/s] near the mid-radius and $x = 0.4$, and higher elsewhere, i.e, more pessimistic. To get the same thermal plasma conditions (and alpha parameters) without ICRH the minimum value of $\chi_{\rm eff}$ must be about 3 [m^2/s] and $\tau_{E,th}(1)$ about 0.52.

The TRANSP sawtooth mixing model is used to helically-mix the current and fast ions at a sawtooth period of 1 sec. This clamps $q_{MHD}(0)$ to remain near 1.0. The sawtooth mixing of the fast alpha particles reduces the alpha parameters in the center, as seen in

Fig. 8c.

0.4 FIRE

FIRE [7] is designed to have normal-conducting magnets, and a double-null divertor geometry. The plasma is assumed to be a standard ELMy H-mode plasma. Profiles of the plasma parameters are shown in Fig. 9. Since the divertors are designed to be coated with beryllium, the dominant impurity species is assumed to be Be with the $Z_{\rm eff}$ profile shown in the Figure. Accumulation of alpha ash is modeled assuming the ash has an anomalous diffusivity of 0.5 m^2/s with no pinch. With the computed alpha thermalization rate and wall recycling rate (20%), the ash accumulates to the steady state profile shown in Fig. 9, which has little impact of depletion on the fusion rate. The confinement time of the ash is computed to be 0.27 s.

The plasma is heated with ICRH at a frequency of 100 MHz to resonate with He^3 on axis. The P_{RF} is 20 MW early, and lowered to 11 MW as the alpha heating increases, to keep $P_\alpha + P_{ext}$ roughly constant. A contour plot showing the power deposition and antenna position is shown in Fig. 10.

The computed value for $\tau_{th,E}(1)$ equals τ_{IPB98y}, but. the enhancement factor given in Eq. 3 would increase τ_{IPB98y} by a factor of 1.6. The computed value for $\chi_{\rm eff}$ is near 3 [m^2/s] near $x = 0.8$, and higher elsewhere. The assumed time evolutions of plasma parameters, motivated by simulations using the TSC code [19], are shown in Fig. 11.

0.5 ITER-FEAT

ITER-FEAT [8,9] is designed to have super-conducting magnets for long pulse duration, and a single-null divertor geometry. The plasma is assumed to be an ELMy H-mode plasma with profiles close to those in Ref. [9] with a target DT fusion yield of $P_{DT} =$ 400 [MW]. Profiles of the plasma parameters are shown in Fig. 12. Accumulation of alpha ash is modeled assuming the ash has an anomalous diffusivity of 0.8 m^2/s with no pinch. With the computed alpha thermalization rate and wall recycling rate (20%), the ash accumulates to the steady state profile shown in Fig. 12, which has little impact of depletion on the fusion rate. The confinement time of the ash is computed to be 1.15 s. The boundary of the plasma is grown from circular to up/down asymmetrically shaped, shown in Fig. 13. The assumed ICRH antenna position and computed contours of the induced E_z are shown in Fig. 14. Time evolutions of plasma parameters are shown in Fig. 15. The sawtooth period is assumed to be 10 s.

The external heating is assumed to consist of 20 MW of ICRH staggered with 33 MW of NBI. This staggering allows study of the heat fluxes and fast ion parameters in three cases with the same assumed plasma profiles: RF-only, RF+NB, and NB-only. The NBI is assumed to consist of 1 MeV (D or T) neutrals from a negative ion-beam system injected in the co-plasma current direction, at a tangency radius of 6 m. This generates a beam-driven current profile that is broad with a total driven current of 1.8 MA. The bootstrap current profile is large near the edge. The effects of both currents on the q_{MHD} profile are shown in Fig. 1.

During the NBI the ratio of the beam and fast alpha density is near unity in the center and increases to 20 near the edge. The average energy of the beam ions in the core is 0.4 MeV, about one-third that of the fast alphas. The slowing down time for the beam ions in the center is 1.15 s, longer than $\tau_{slow}(0)$ of the fast alpha particles. This indicates that the NBI would interfere with attempts to measure alpha effects.

The ICRH is assumed to be 53 MHz for He^3 on axis. The ICRH minority He^3 ions will not have high energy, and thus should not be a complication in studying fast alpha effects (and conversely, will not contribute to stabilizing sawteeth or TAE). Their tail temperature, $T_{min}(0)$ defined by $(2/3)\mathrm{W}_{min,\ perp}(0)/n_{min}(0)$, is close to T_i, as shown in Table 2.

The value of $\tau_{E,th}(1)$ is slightly below the τ_{IPB98y} value. With the choice of a flat n_e profile, the form factor in Eq. 3 reduces $\tau_{E,th}$ by a factor of 0.81. Since the profiles are held fixed during the flattop phase as the heating power changes, χ_{eff} changes. The minimum values during the phase of maximum heating (20 MW ICRH, 33 MW NNBI, and 75 MW alpha) is 5 $[m^2/s]$. The minimum drops to 4.5 $[m^2/s]$ after the ICRH is shut off and later to 3 $[m^2/s]$ after the NBI is shut off. If χ_{eff} were held constant in time, the stored energy would change as the heating changed.

Alpha parameters have been calculated [20] for two ITER-EDA plasmas producing 1.5 GW fusion power. One had a nearly flat electron density profile, similar to the one used here for ITER-FEAT. The other had a relatively peaked n_e. The values for the alpha parameters calculated in the flat profile case are very similar to those given in Table 1.

5. Summary and Discussion

This paper reports results from TRANSP analysis of five plasmas with high DT fusion yield. The TFTR and JET plasmas achieved modest values of P_{DT}, helping to establish the scientific feasibility of energy production in future Tokamak reactors. Three examples of plasmas from the proposed next step Tokamaks with much higher P_{DT} are analyzed. The results of this study include electronic files of the equilibria, plasma parameters, and alpha parameters for use in studies of alpha effects and MHD and microturbulence instabilities.

The assumed plasma conditions are similar to examples proposed by proponents of the three next step Tokamaks. The assumed plasma profiles and computed heat deposition profiles give values of $\tau_{E,th}(1)$ close to the L-mode scaling in the case of Ignitor and close to the ELMy H-mode fits (Eqs. 1, 3) in the cases of FIRE and ITER-FEAT. It would be useful to use physics-based and empirical models to predict plasma profiles that can be sustained by the heating and fueling sources.

There are a number of interesting similarities and expected differences between the TFTR and JET plasmas and those considered for the next step burning plasma experiments in IGNITOR, FIRE, and ITER. Similarities include the values of $\beta_\alpha(0), v_\alpha(0)/v_{Alfven}(0)$, and $\max\{-R \times \nabla(\beta_\alpha)\}$, which vary by a factor of at most four for the five plasmas. The value of $\max\{P_\alpha/P_{heat}\}$ varies by only a factor of 4.5.

One major difference is that $T_i >> T_e$ in the center of TFTR and JET plasmas, whereas they are assumed to be nearly equal in the next step Tokamak plasmas, as is expected since the energy equilibration should be fast at higher density. Another difference is that the TFTR and JET plasmas have large toroidal rotation rates due to the intense NBI (with central Mach numbers of the carbon impurity being 0.25 and 1.6 respectively), whereas the next step plasmas are expected to have very low rotation rates due to the difficulty (cost) of injecting momentum into a Tokamak reactor. Both $T_i >> T_e$ and large rotation rates are correlated with high confinement in present-day experiments.

Another difference is that the slowing down times for the alpha particles (τ_{slow}) is small compared to the thermal energy confinement times in the burning plasmas, unlike the situation in the achieved experiments.

Issues for future investigation include checking the MHD and micro-instability of the plasmas assumed for the next step Tokamaks. For instance, the instability to ITG modes depends sensitively on the temperature gradients. If the plasmas are instable, the pedestal temperatures may have to be increased to reduce the gradients while keeping the central values high enough for high P_{DT}. It appears that the temperature at the separatrix should be below 1 [keV] to prevent excessive sputtering erosion of surfaces down stream in the divertor [21]. These constraints suggest the need for a large decrease in T_i between the top and bottom of the pedestal. Experiments in JET suggest that if there is a large decrease in the pedestal, the ELMs would be Type I with excessive losses of energy in each ELM [22]. Gyrokinetic analysis of JET ELMy H-mode plasmas indicates that when the flow shear and linear microturbulence growth rates near the top of the pedestal are comparable, the energy confinement remains good [23]. This suggests that driving large flow shear in next step Tokamaks might permit high confinement and central temperatures with low pedestal temperatures.

6. Acknowledgment

This work was supported in part by the US DoE Contract No. DE-AC02-76CH03073.

References

[1] C. Angioni, A. Pochelon, N.N. Gorelenkov, *et al.*, to be published in PPCF.
[2] F. Porcelli, D. Boucher, and M.N. Rosenbluth, PPCF **38**, 2163 (1996).
[3] G.F. Fu, C.Z. Chen, N. Gorelenkov, *et al.*, Phys. of Plasmas, **3**, 4036 (1996).
[4] R.V. Budny, M.G. Bell, A.C. Janos, *et al.*, Nucl. Fusion **35**, 1497 (1995), and references therein.
[5] N. Gorelenkov, C.Z. Chang, and W.M. Tang, Phys. of Plasmas **5**, 3389 (1998).
[6] http://www.frascati.enea.it/ignitor/; A. Airoldi, G. Cenacchi, Nucl. Fusion **41**, 687 (2001); B. Coppi, A. Aroldi, F. Bombarda, *et al.*, Nucl. Fusion **41**, 1253 (2001); A. Airoldi, G. Cenacchi, Nucl. Fusion **37**, 1117 (1997).
[7] http://fire.pppl.gov
[8] http://www.itereu.de
[9] D.J. Campbell, Phys. Plasmas **8**, 2041 (2001)
[10] M.G. Bell, S. Batha, M. Beer, *et al.*, Phys. of Plasmas **4**, 1714 (1997)
[11] M. Keilhacker, A. Gibson, C. Gormezano, P.J. Lomas, *et al.*, Nucl. Fusion **39**, 209 (1999).
[12] R.J. Goldston, D.C. McCune, H.H. Towner, S.L. Davis, *et al.*, J. Comput. Phys. **43**, 61 (1981).
[13] S.S. Medley, R.V. Budny, H.H. Duong, R.K. Fisher, *et al.*, Nucl. Fusion **38**, 1283 (1998).
[14] G.A. McKee, *et al.*, Nucl. Fusion **37**, 501 (1997).
[15] M. Evrard, J. Ongena, and D. van Eester, "Improved Dielectric Tensor in the ICRH module of TRANSP", in AIP Conference Proceedings **335**, Radio-Frequency Power in Plasmas, 11th topical conference, Palm Springs, 235 (1995).
[16] ITER Physics Basis, Nucl. Fusion **39**, 2204 (1999).
[17] J.G. Cordey, D.C. McDonald, K. Borrass, *et al.*, P3.011 in Proc. 28th EPS Conference on Controlled Fusion and Plasma Physics, Madeira, Portugal, 2001. ECA **25A**, 969.
[18] S.E. Sharapov, D. Borba, A. Fasoli, *et al.,* Nucl. Fusion **39**, 373 (1999).
[19] S.C. Jardin, N. Pomphery, and J. Delucia, J. Comput. Phys., **46**, 481 (1986).
[20] R.V. Budny, D.C. McCune, M.H. Redi, *et al.,* Phys. of Plasmas **3**, 4583 (1996).
[21] P.C. Stangeby, **The Plasma Boundary of Magnetic Fusion Devices**, Institute of Physics Publishing (Bristol and Philadelphia, 2000)p 232.
[22] A. Loarte, M. Bécoulet, G. Saibene, *et al.*, P3.005, Proceedings of the 28th EPS conference, Madeira, 2001, ECA **25A**, 945.
[23] R.V. Budny, B. Alper, D.N. Borba, J.G. Cordey,*et al.,* Nucl. Fusion, **42**, 66 (2002).

Tokamak:	TFTR	JET	IGNITOR	FIRE	ITER
RUNID	80539A24	42976C10	30000B16	50000A10	03000A18
time	3.76	13.35	6.5	20.0	180.0
R [m]	2.52	2.92	1.32	2.14	6.2
a [m]	0.87	0.94	0.48	0.60	2.0
κ (1)	1.02	1.80	1.80	2.00	1.85
δ (1)	0.02	0.35	0.40	0.49	0.49
P_{vol} $[m^3]$	38.8	84.0	9.9	27.2	820
B_{Tor} [T]	5.5	3.82	13.1	10.0	5.28
I_p [MA]	2.66	4.0	11.0	7.7	15.0
I_{boot} [MA]	0.65	0.40	0.90	1.9	2.1
$q_{MHD}(1)$	4.05	4.7	3.5	4.0	3.8
A_h	2.20	2.53	2.5	2.5	2.5
$T_e(0)$ [keV]	13.2	11.0	9.9	11.9	23.5
$T_i(0)$ [keV]	40.0	23.0	9.9	11.9	19.5
$< T_i >$ [keV]	8.7	7.3	5.4	7.2	8.6
$n_e(0)[10^{20}/m^3]$	1.02	0.45	9.4	4.9	1.02
$< n_e > [10^{20}/m^3]$	0.40	0.48	3.5	3.4	0.99
$\bar{n}_e/\bar{n}_{Greenwald}$	0.46	0.32	0.35	0.59	0.84
$Z_{eff}(0)$	3.1	1.5	1.2	1.39	1.54
$< \beta_{total} > (\%)$	1.03	2.17	1.10	2.10	2.70
$< \beta_{thermal} > (\%)$	0.60	1.79	1.07	2.00	2.45
β_n	1.85	1.95	0.63	1.63	1.90
W_{tot} [MJ]	7.5	17.0	11.6	35.0	370
P_{DT} [MW]	10.3	15.8	78	152	408
P_{ext} [MW]	41.6	25.4	24.8	12.4	33
$P_{\alpha-el}$ [MW]	1.1	2.1	13.1	24.9	59
$P_{\alpha-ion}$ [MW]	0.1	0.3	2.7	5.7	23
P_α [MW]	1.2	2.4	14.9	30.0	83
P_{heat} [MW]	27.0	16.4	45.0	42.6	117
$W_{tot}/(P_\alpha + P_{ext})$ [sec]	0.18	0.61	0.29	0.83	3.16
$\tau_{E,th}(1)$ [sec]	0.13	0.59	0.25	0.79	2.85
τ_{IPB98y} [sec]	0.14	0.55	0.42	0.79	3.10
τ_L [sec]	0.066	0.30	0.19	0.40	1.35
$\tau_{slow}(0)$ [sec]	0.48	1.0	0.043	0.097	0.86
$\tau_{scat}(0)$ [sec]	5.8	21	1.6	2.6	11.0
$P_\alpha(0)$ [MW/m^3]	0.28	0.08	14.1	5.0	0.43
$\max\{P_\alpha/P_{heat}\}$	0.20	0.23	0.62	0.83	0.90
$n_\alpha(0)/n_e(0)$ (%)	0.17	0.28	0.12	0.18	0.55
$\beta_\alpha(0)$ (%)	0.30	0.4	0.27	0.30	0.70
$< \beta_\alpha > (\%)$	0.034	0.1	0.021	0.060	0.17
$max\{-R \times \nabla(\beta_\alpha)\}$ (%)	2.0	2.3	0.8	1.3	5.0
$v_\alpha(0)/v_{Alfven}(0)$	1.72	2.52	2.04	1.60	1.80

Table 1: *Summary of plasma parameters*

Tokamak:	JET	IGNITOR	FIRE	ITER
RUNID	42976C10	30000B16	50000A10	03000A17
time	13.35	7.5	20.0	140.0
ICRH frequency [MHz]	51.2-56.5	120, 140	100	53
ICRH power [MW]	3.4	24	11.2	20
minority ion	H	He^3	He^3	He^3
n_{min}/n_e %	2.0	2.0	2.0	3.0
$T_{min}(0)$ [keV]	150	≈40	10.2	17.0
P_{RF-min}/P_{RF} %	60	59	60	44
P_{RF-T}/P_{RF} %	1	11	10	5
P_{RF-D}/P_{RF} %	17	5	2	4
P_{RF-e}/P_{RF} %	13	24	26	36

Table 2: *Summary of ICRH parameters*

Figure Captions

Fig. 1 - Profiles of q_{MHD} in the TFTR, JET, IGNITOR, FIRE, and ITER plasmas at the times of analysis.
Fig. 2 - Profiles of the TFTR supershot before the carbon bloom,
Fig. 3 - Time evolution of parameters in the TFTR supershot. The measured $T_i(0)$ (for carbon) became unrealistically low after the density became too high for good beam penetration. $P_{fast\ ion}$ is the heating power of the thermal plasma from the NBI and alphas. E_α is the average energy of the fast alphas in the core.
Fig. 4 - Profiles of the JET hot-ion H-mode plasma before the series of giant ELMs.
Fig. 5 - Time evolution of parameters in the JET plasma.
Fig. 6 - Assumed profiles of the IGNITOR plasma in the flattop phase.
Fig. 7 - Contours of the ICRH-induced Re$\{E_r\}$ in the IGNITOR plasma.
Fig. 8 - Time evolution of parameters in the IGNITOR plasma.
Fig. 9 - Profiles of the FIRE plasma in the flattop phase. The he^4 ash density, computed from the fast alpha thermalization and assumed 20% wall recycling source rates using an explicit diffusivity of 0.5 $[m^2/s]$, is in steady state at the time shown.
Fig.10 - Contours of ICRH-induced Re$\{E_r\}$ in the FIRE plasma.
Fig.11 - Time evolution of parameters in the FIRE plasma. The alpha parameters in c) are volume-averaged out to the $x = 0.1$ flux surface to reduce Monte Carlo fluctuations.
Fig.12 - Assumed profiles of the ITER plasma The he^4 ash density, computed from the fast alpha thermalization and assumed 20% wall recycling source rates using an explicit diffusivity of 0.8 $[m^2/s]$, is in steady state at the time shown.
Fig.13 - Assumed boundary for the ITER plasma
Fig.14 - Contours of the ICRH-induced Re$\{E_r\}$ in ITER-FEAT
Fig.15 - Time evolution of parameters in the ITER plasma. The alpha parameters in c) are volume-averaged out to the $x = 0.1$ flux surface to reduce Monte Carlo fluctuations.

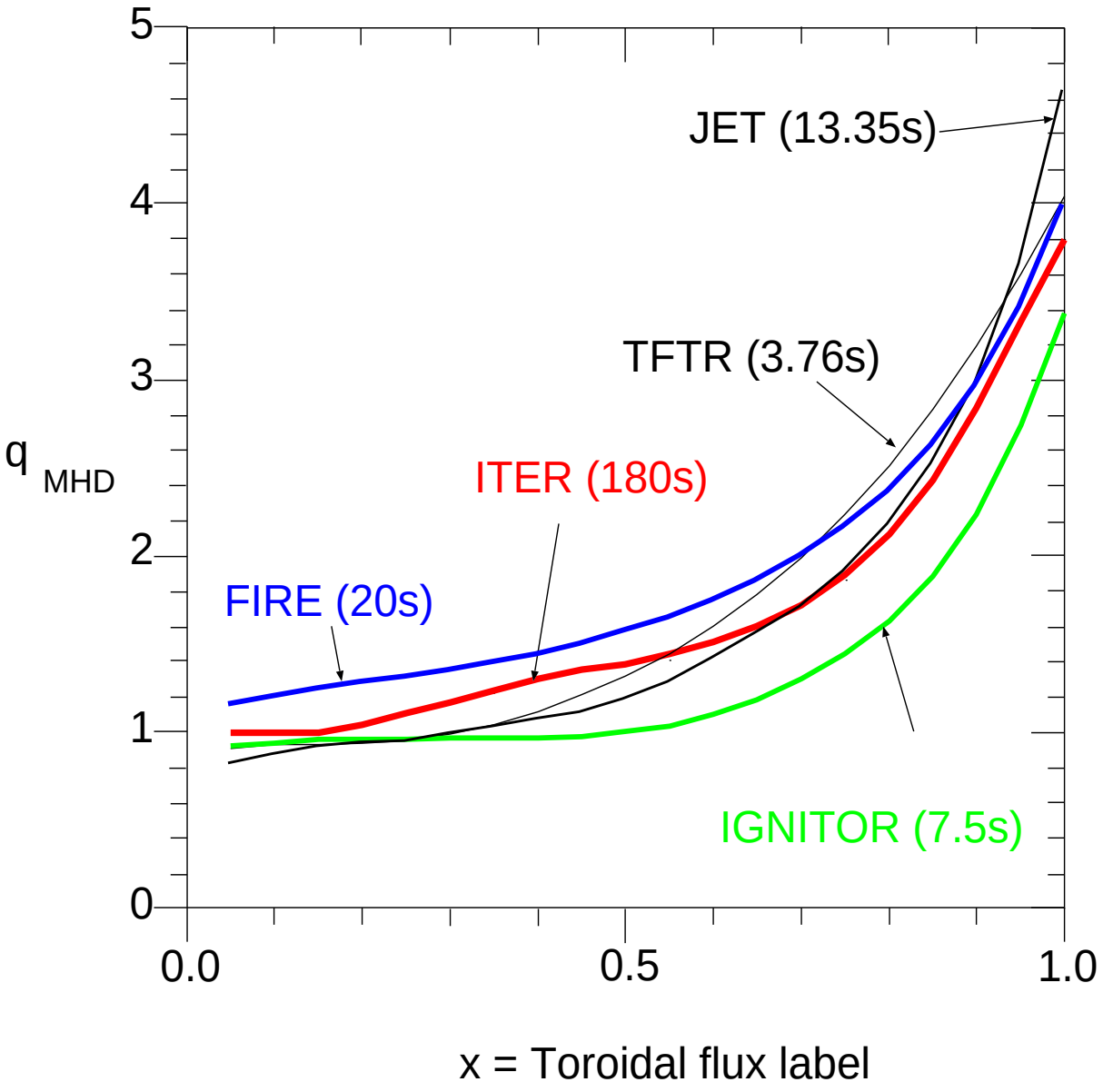
5
4
3
2
1
0
0.0
0.5
1.0
q MHD
JET (13.35s)
TFTR (3.76s)
ITER (180s)
FIRE (20s)
IGNITOR (7.5s)
x = Toroidal flux label

Figure 1:

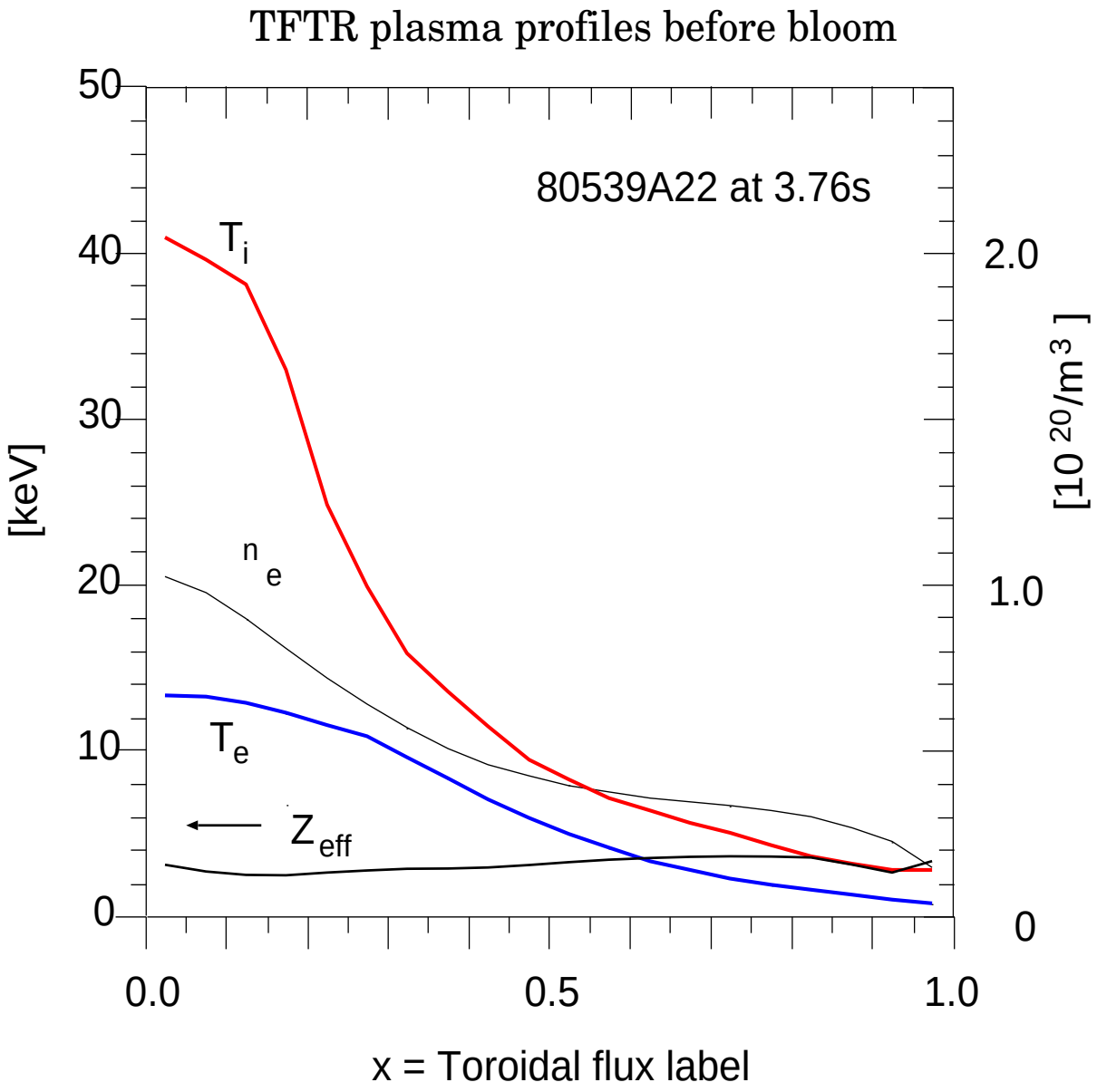
TFTR plasma profiles before bloom
80539A22 at 3.76s
T_i
n_e
T_e
Z_eff
[keV]
[10^20/m^3]
50
40
30
20
10
0
2.0
1.0
0
0.0
0.5
1.0
x = Toroidal flux label

Figure 2:

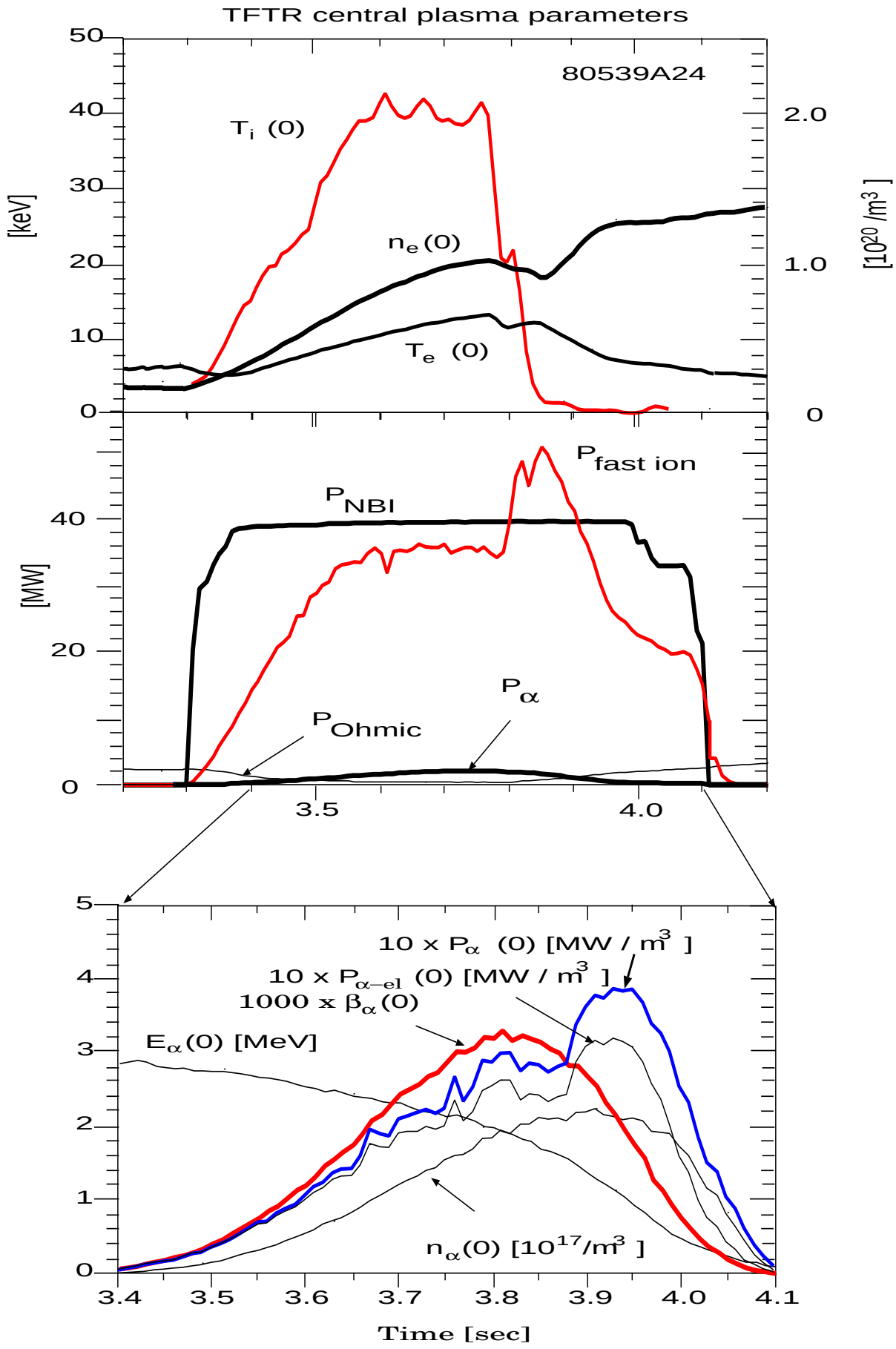
TFTR central plasma parameters
80539A24
T_i (0)
n_e(0)
T_e (0)
[keV]
[10^{20} /m^3]
$P_{fast\ ion}$
P_{NBI}
P_{Ohmic}
P_α
[MW]
10 x P_α (0) [MW / m^3]
10 x $P_{\alpha-el}$ (0) [MW / m^3]
1000 x β_α(0)
E_α(0) [MeV]
n_α(0) [10^{17}/m^3]
Time [sec]

Figure 3:

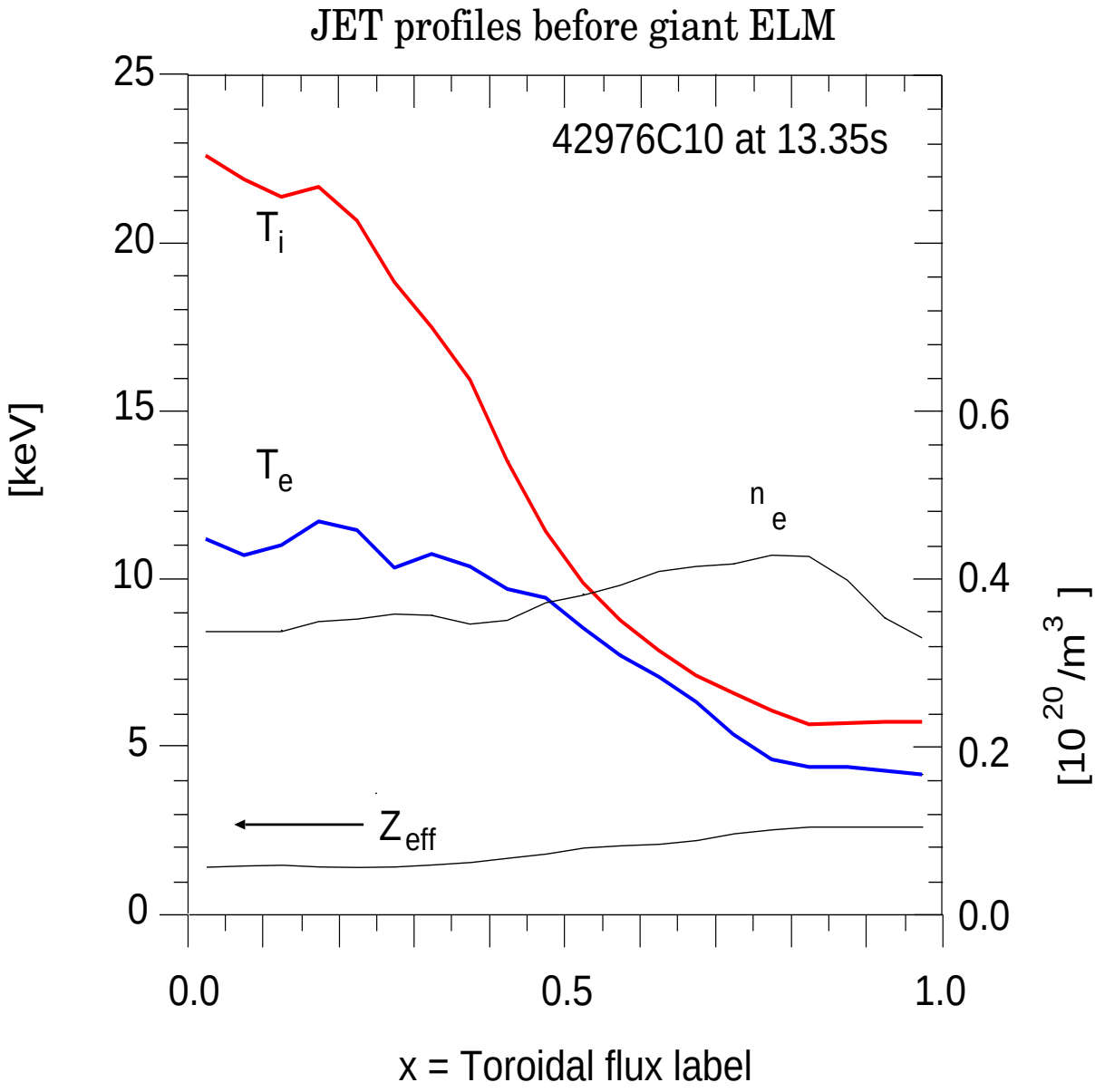
JET profiles before giant ELM
42976C10 at 13.35s
T_i
T_e
n_e
Z_{eff}
[keV]
$[10^{20}/m^3]$
25
20
15
10
5
0
0.6
0.4
0.2
0.0
0.0
0.5
1.0
x = Toroidal flux label

Figure 4:

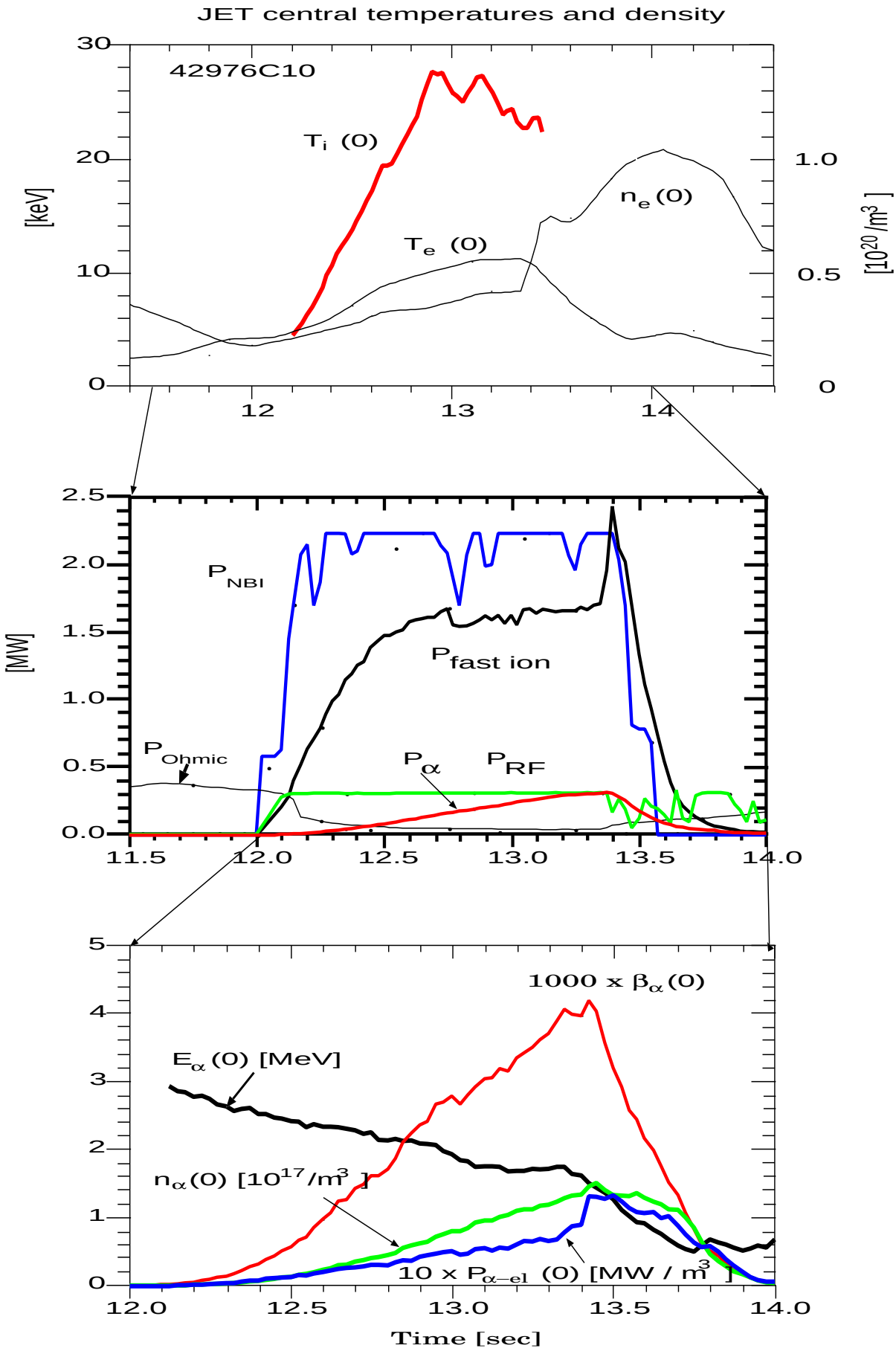
JET central temperatures and density
42976C10
T_i (0)
T_e (0)
n_e (0)
[keV]
$[10^{20}/m^3]$
P_{NBI}
$P_{fast\ ion}$
P_{Ohmic}
P_α
P_{RF}
[MW]
$1000 \times \beta_\alpha(0)$
E_α (0) [MeV]
$n_\alpha(0)$ $[10^{17}/m^3]$
$10 \times P_{\alpha-el}$ (0) [MW / m^3]
Time [sec]

Figure 5:

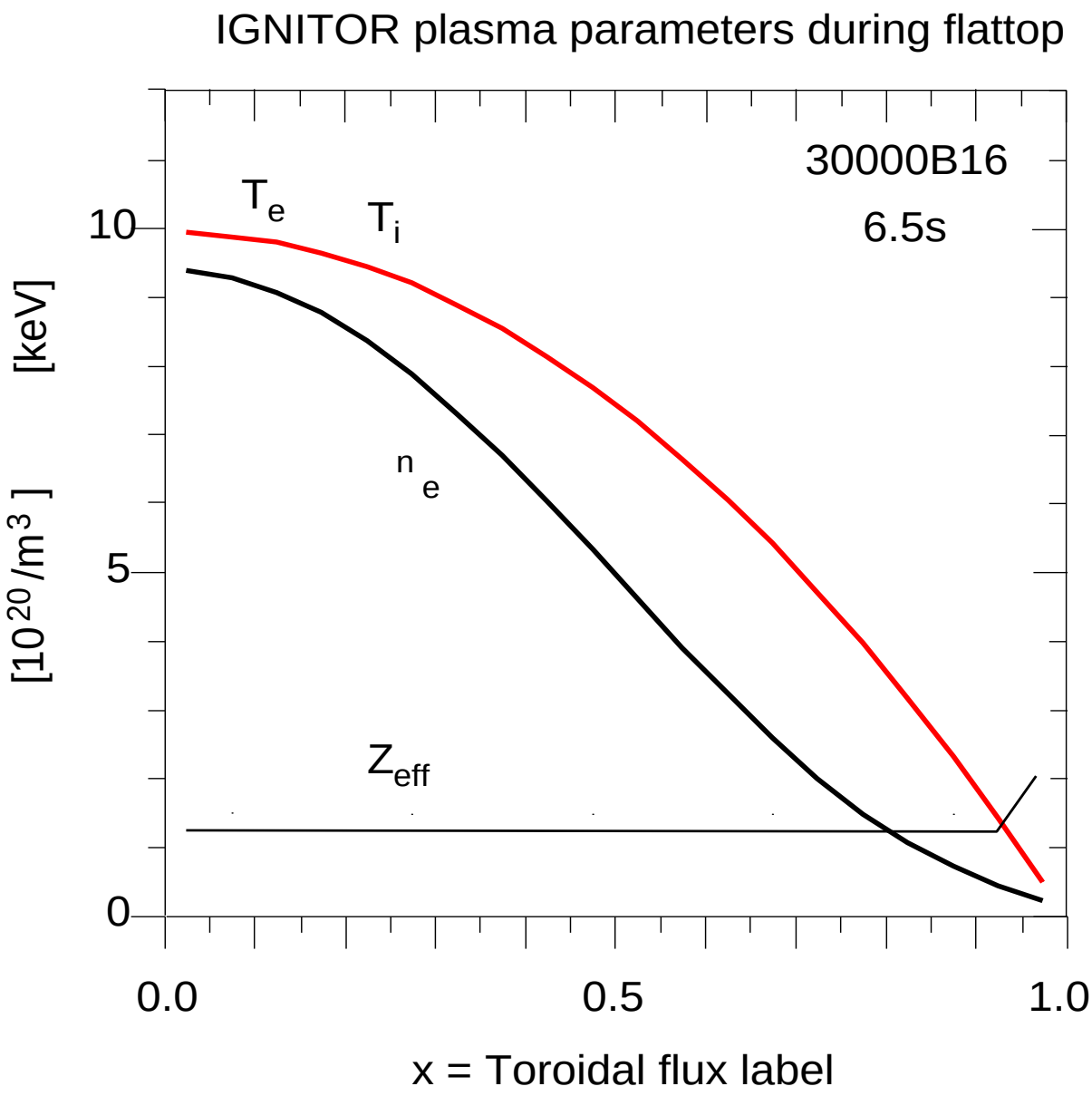
IGNITOR plasma parameters during flattop
30000B16
6.5s
T_e
T_i
n_e
Z_{eff}
10
5
0
0.0
0.5
1.0
[keV]
[10^{20}/m^3]
x = Toroidal flux label

Figure 6:

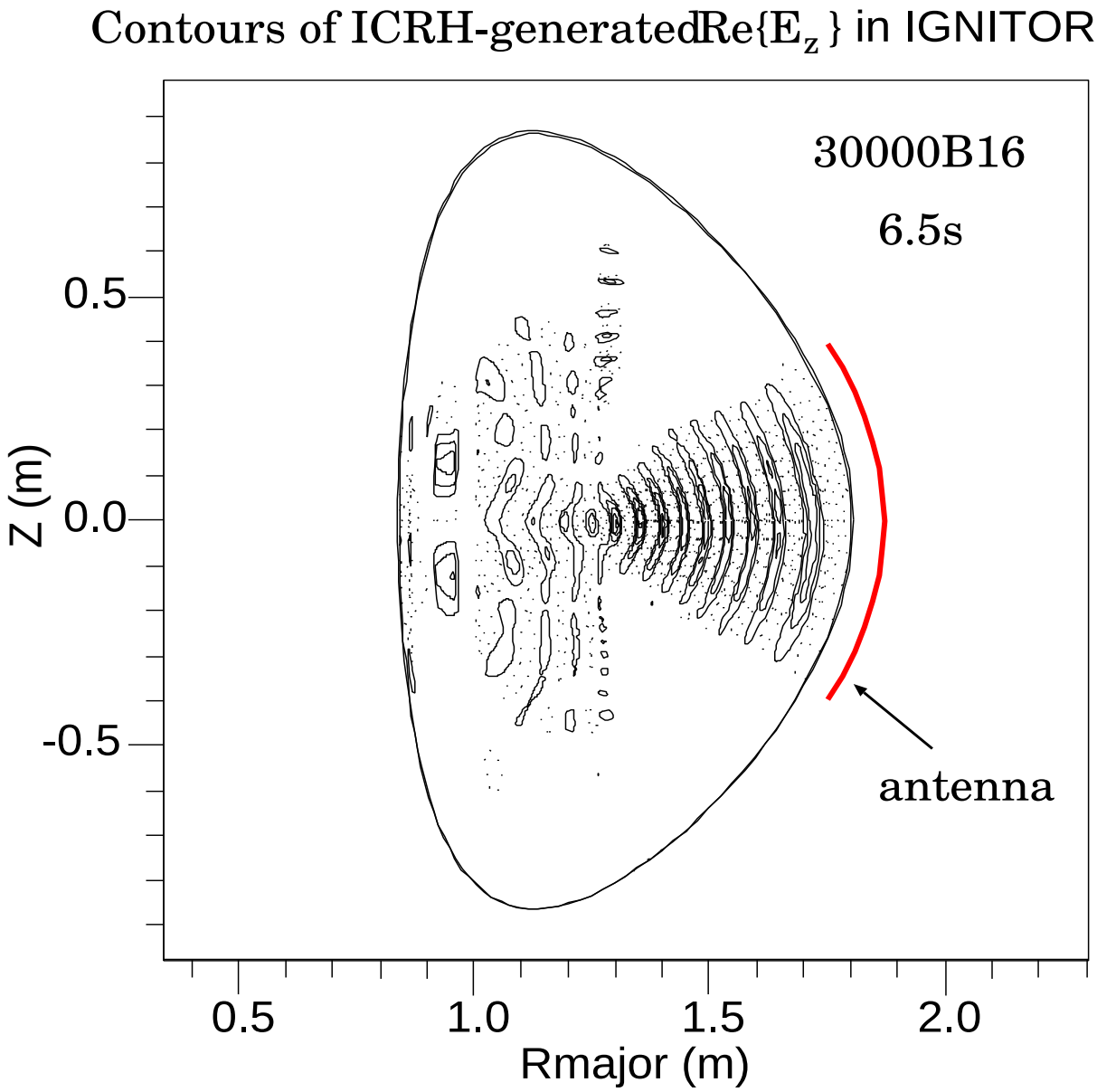
Contours of ICRH-generatedRe{E$_z$} in IGNITOR
30000B16
6.5s
antenna
Z (m)
0.5
0.0
-0.5
0.5
1.0
1.5
2.0
Rmajor (m)

Figure 7:

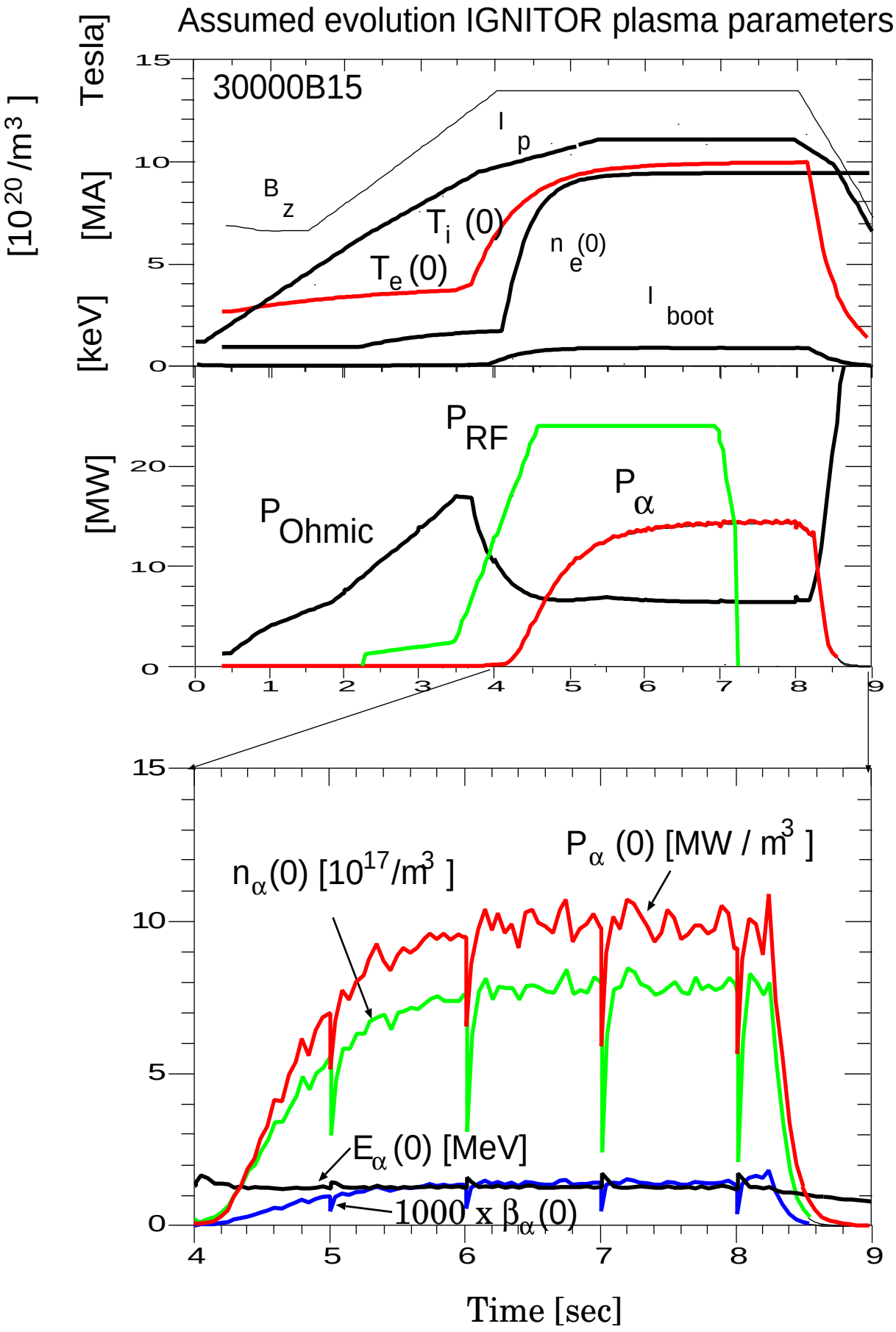
Assumed evolution IGNITOR plasma parameters
30000B15
Tesla]
[MA]
[keV]
[10^20/m^3]
[MW]
B z
I p
T i (0)
T e (0)
n e(0)
I boot
P RF
P α
P Ohmic
n α(0) [10^17/m^3]
P α (0) [MW / m^3]
E α (0) [MeV]
1000 x β α (0)
Time [sec]

Figure 8:

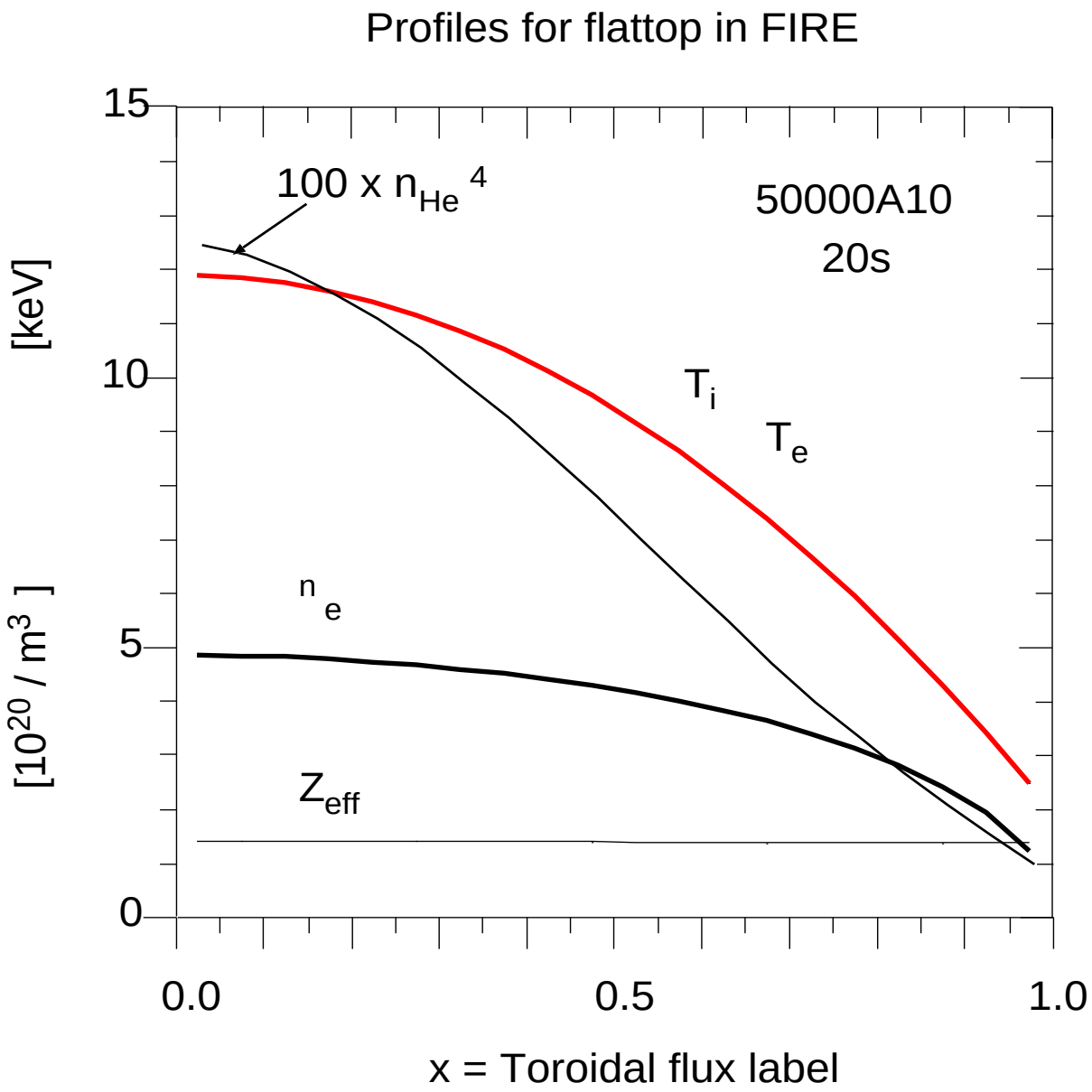
Profiles for flattop in FIRE
15
10
5
0
[keV]
[10^20 / m^3]
100 x n_He 4
50000A10
20s
T_i
T_e
n_e
Z_eff
0.0
0.5
1.0
x = Toroidal flux label

Figure 9:

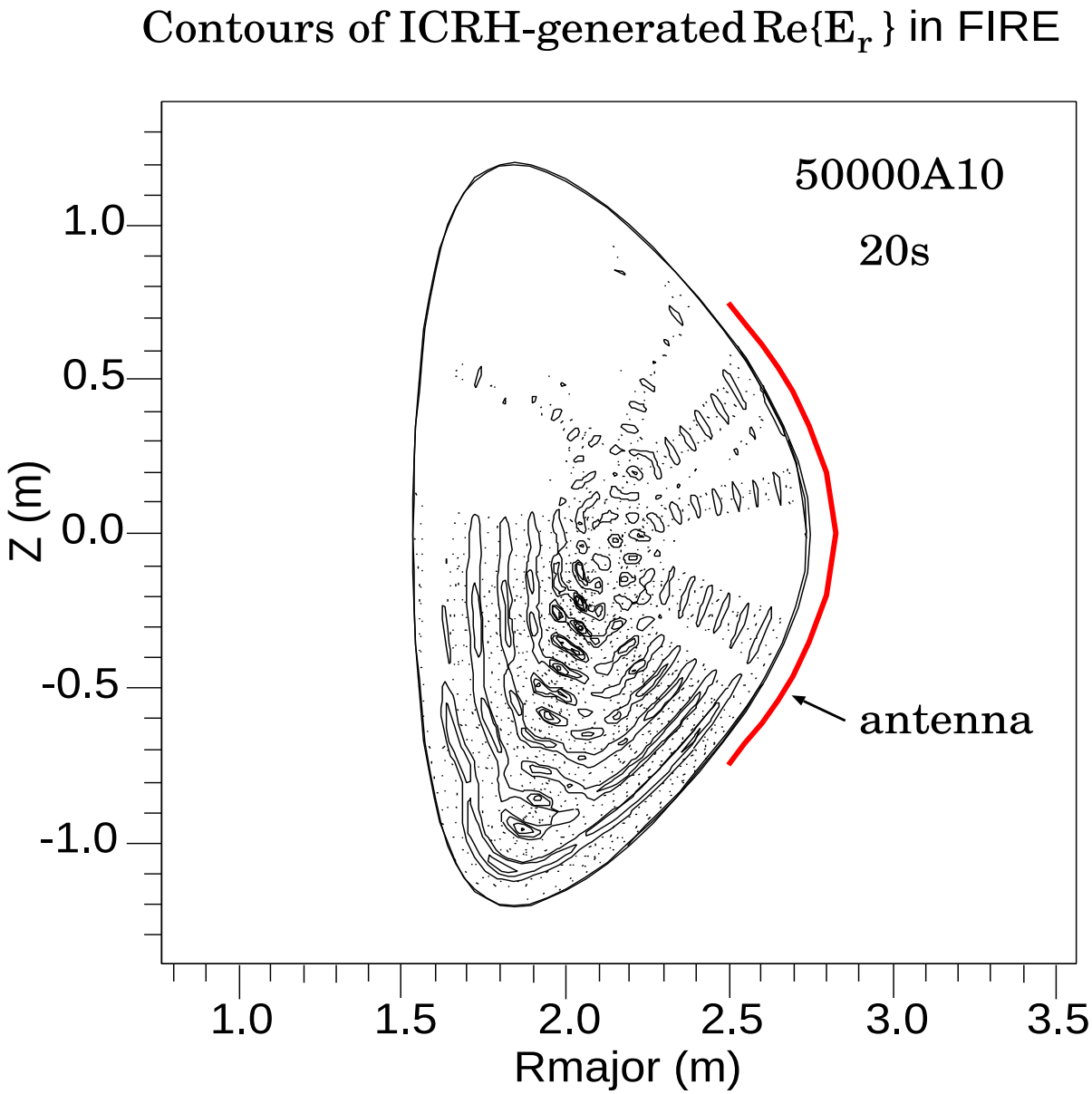
Contours of ICRH-generated Re{E_r} in FIRE
50000A10
20s
antenna
Z (m)
1.0
0.5
0.0
-0.5
-1.0
1.0
1.5
2.0
2.5
3.0
3.5
Rmajor (m)

Figure 10:

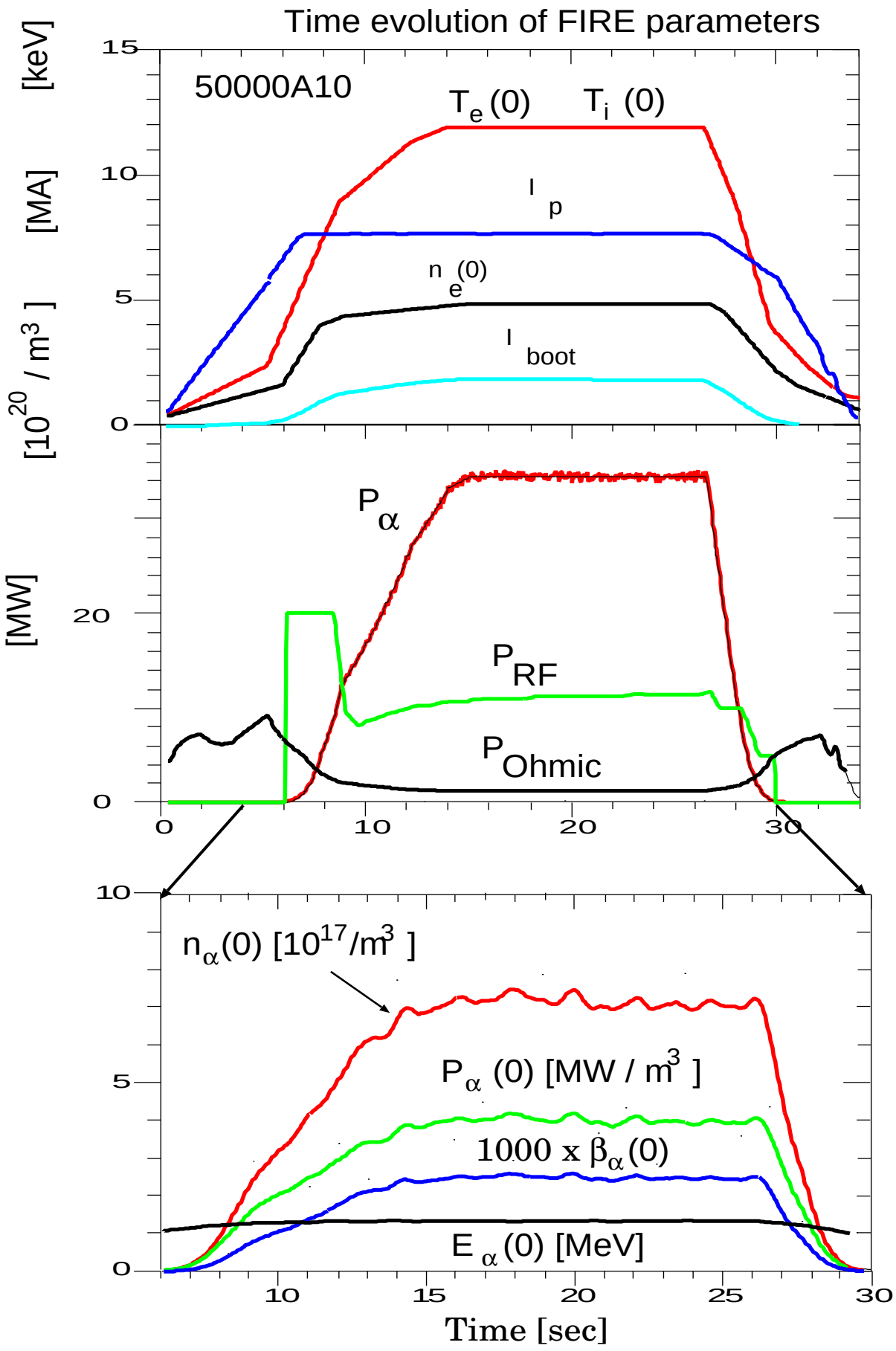
Time evolution of FIRE parameters
50000A10
$T_e(0)$ $T_i(0)$
I_p
$n_e(0)$
I_{boot}
[keV]
[MA]
[10^{20} / m^3]
P_α
P_{RF}
P_{Ohmic}
[MW]
$n_\alpha(0)$ [$10^{17}/m^3$]
P_α (0) [MW / m^3]
1000 x $\beta_\alpha(0)$
$E_\alpha(0)$ [MeV]
Time [sec]

Figure 11:

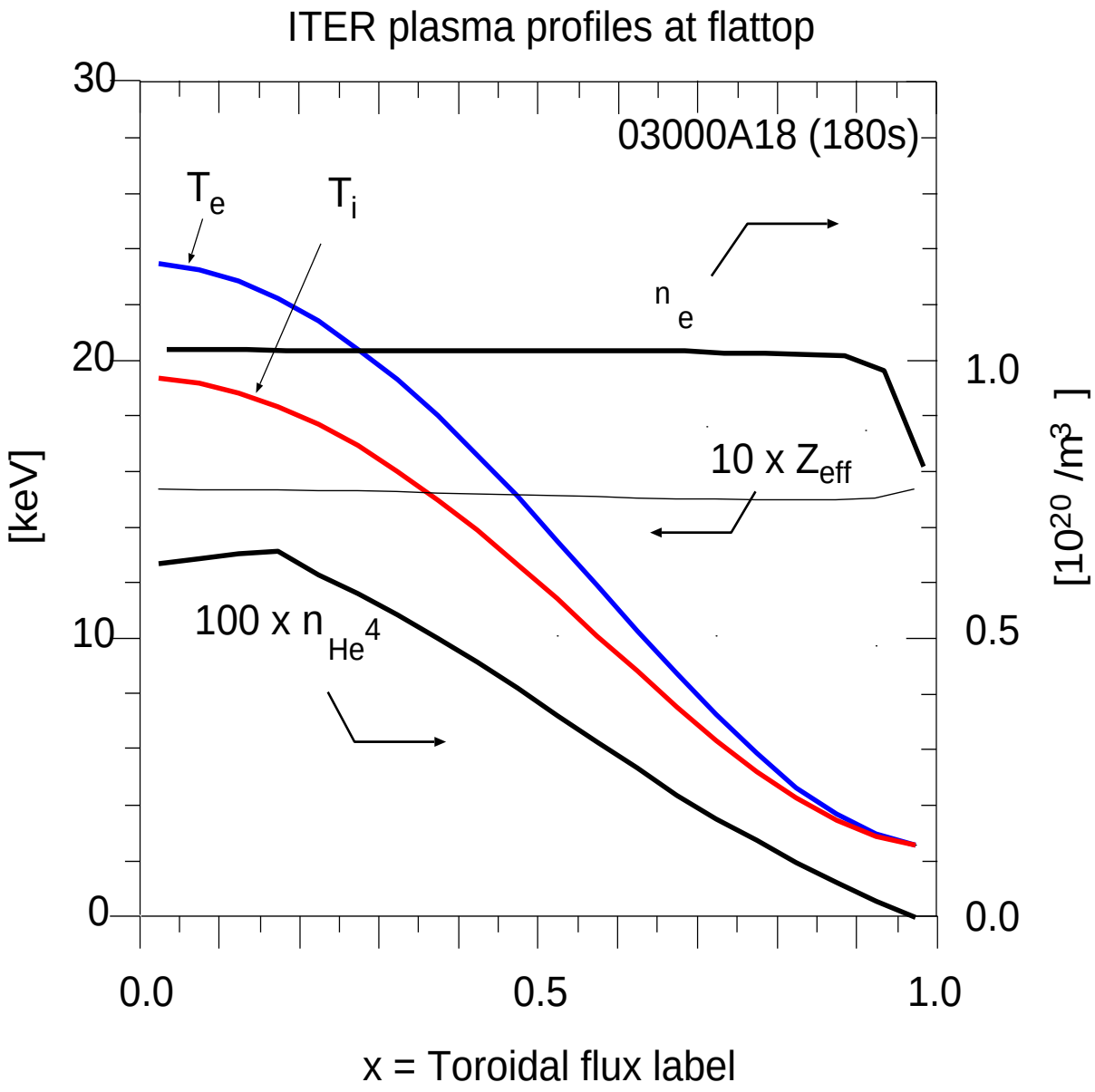
ITER plasma profiles at flattop
03000A18 (180s)
T_e
T_i
n_e
10 x Z_eff
100 x n_He4
[keV]
[10^20 /m^3]
30
20
10
0
1.0
0.5
0.0
0.0
0.5
1.0
x = Toroidal flux label

Figure 12:

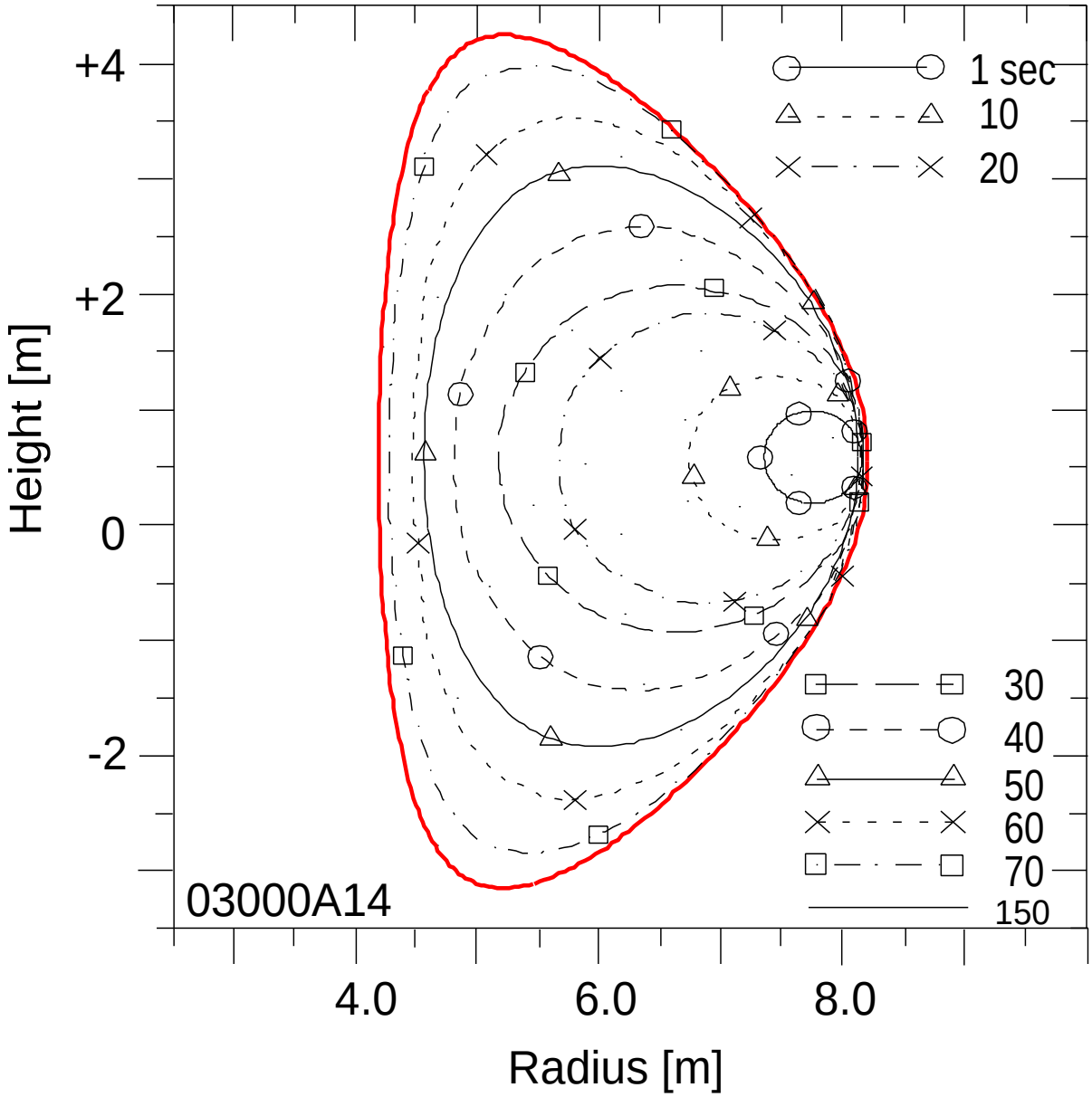
+4
+2
0
-2
Height [m]
4.0
6.0
8.0
Radius [m]
1 sec
10
20
30
40
50
60
70
150
03000A14

Figure 13:

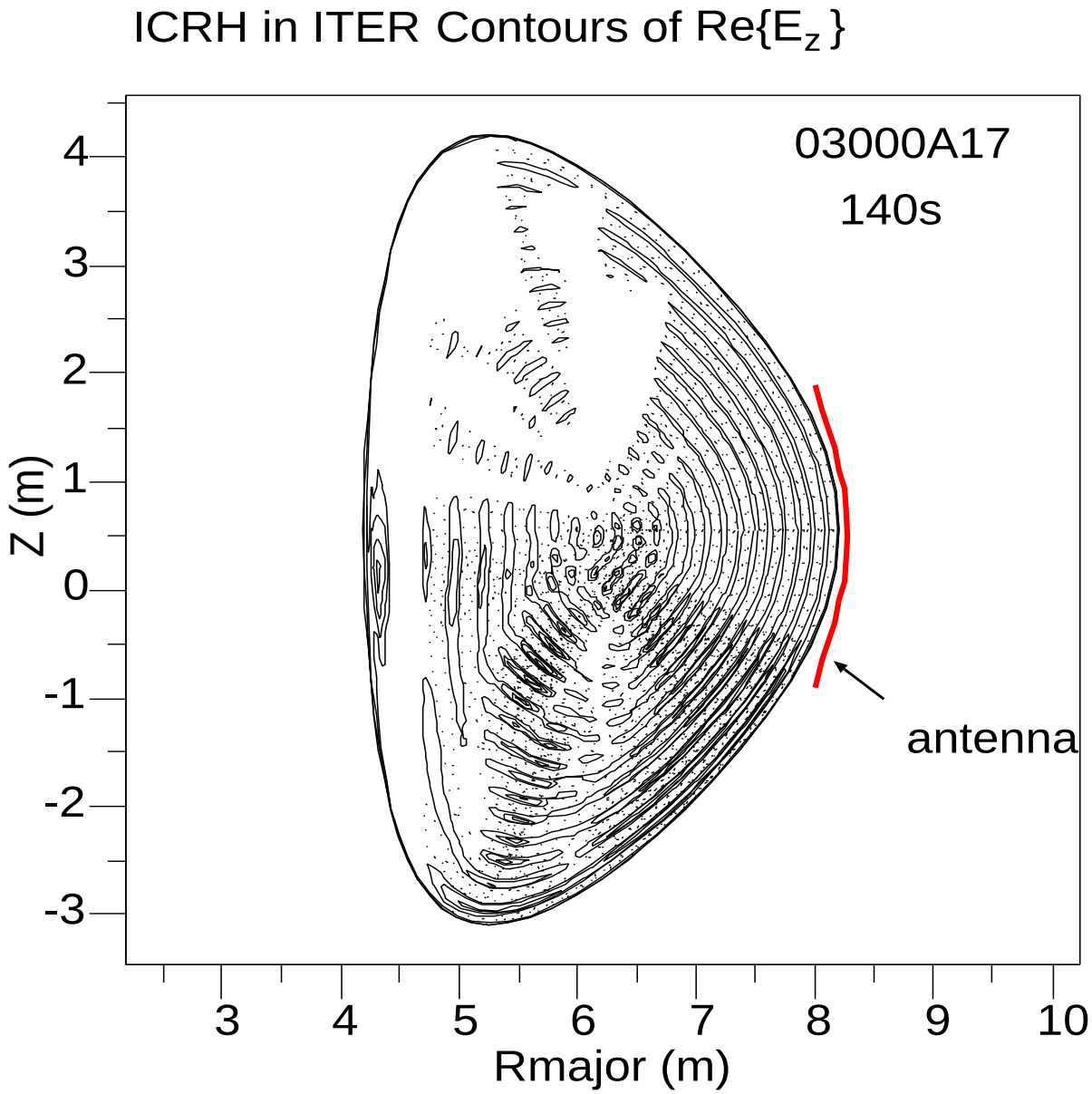
ICRH in ITER Contours of Re{E_z}
03000A17
140s
antenna
Z (m)
Rmajor (m)
4
3
2
1
0
-1
-2
-3
3
4
5
6
7
8
9
10

Figure 14:

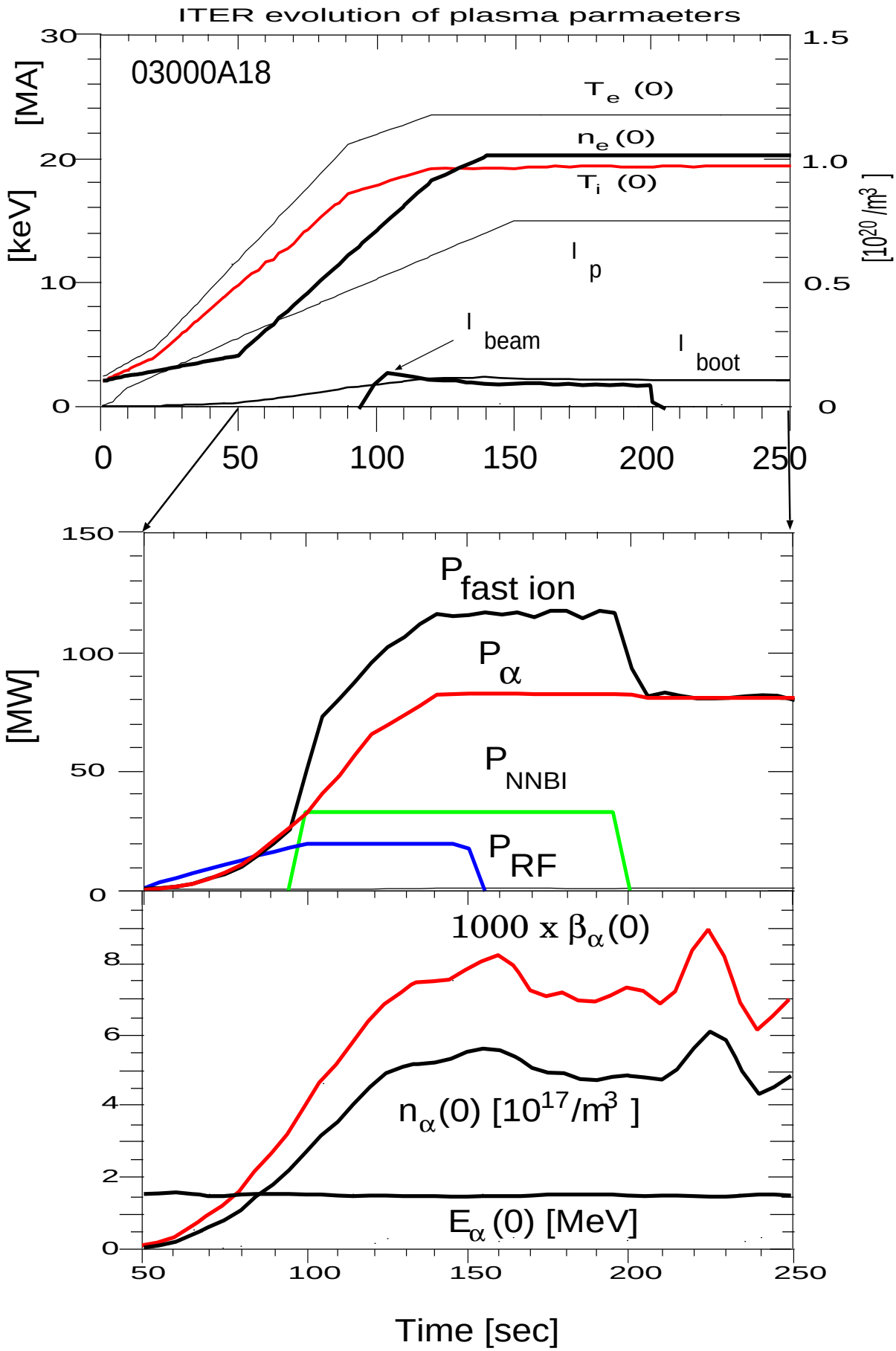
ITER evolution of plasma parmaeters
03000A18
[MA]
[keV]
[10^20 /m^3]
T_e (0)
n_e (0)
T_i (0)
I_p
I_beam
I_boot
P_fast ion
P_α
P_NNBI
P_RF
[MW]
1000 x β_α(0)
n_α(0) [10^17/m^3]
E_α (0) [MeV]
Time [sec]

Figure 15: